

Estimation of the Charge Mobility of Phenanthroline derivatives with the view of Density Functional Theory: Reorganization Energy and Charge Transfer Integral are in play

Zeynep Türkmen Bulca¹, Gül Yakalı^{2*}

¹ Nanoscience and Nanotechnology Program, Institute of Science, Izmir Katip Çelebi University, Izmir, Turkey

² Department of Engineering Sciences, Faculty of Engineering, Izmir Katip Çelebi University, Izmir, Turkey

*Correspondence: gul.yakali@ikcu.edu.tr

Abstract

Molecular arrangement and noncovalent interactions in organic materials greatly influence the charge mobility in organic light-emitting diodes (OLEDs), organic photovoltaics (OPVs), and organic field-effect transistors (OFETs). In the light of the this argument, we examined the electronic properties of the phenanthroline derivatives by considering the charge mobility with the combination of density functional theory and Marcus Charge Transfer Theory. The drift electron mobility of the molecule **1** and **2** were determined to $21.13 \text{ cm}^2 \text{ V}^{-1} \text{ s}^{-1}$ and $18.00 \text{ cm}^2 \text{ V}^{-1} \text{ s}^{-1}$, respectively through J type $\pi \cdots \pi$ stacking interactions created by small perpendicular distances between the adjacent rings. The effective charge pathways of the molecules were generated with strong $\pi \cdots \pi$ stacking interactions consolidated by noncovalent interactions in their solid phases. The electron reorganization energy for both molecules were determined smaller than that of holes which means they have n-type semiconductor properties. The charge transfer integrals were calculated with the optimization of molecules' dimer configurations that the theoretical results demonstrate the charge transfer integral depends on the distance between the stacking rings. High charge transfer integral and small reorganization energy give the high charge mobility for the semiconductor molecules. Beside the mobility, energy band gap, ionization potential, electron and hole injection barriers of the molecules were interpreted to further understand their electronic properties. Due to the small LUMO values which provide n-type molecule and small electron injection barrier. From our work both molecules can be effective n type organic semiconductor devices with the high mobility and can be modified for more efficient charge transport in phenanthroline derivatives.

Article History

Received 22.05.2023

Accepted 17.02.2024

Keywords

n-type organic semiconductor devices, DFT, J type $\pi \cdots \pi$ stacking, charge mobility, phenanthroline derivatives.

1. Introduction

Molecular arrangement and noncovalent interactions in organic materials greatly influence the charge mobility in organic light-emitting diodes (OLEDs), organic photovoltaics (OPVs), and organic field-effect transistors (OFETs). In the light of this argument, we examined the electronic properties of the phenanthroline derivatives by considering the charge mobility with the combination of density functional theory and Marcus Charge Transfer Theory. The drift electron mobility of the molecule **1** and **2** were determined to 21.13 cm² V⁻¹ s⁻¹ and 18.00 cm² V⁻¹ s⁻¹, respectively through J type $\pi \cdots \pi$ stacking interactions created by small perpendicular distances between the adjacent rings. The effective charge pathways of the molecules were generated with strong $\pi \cdots \pi$ stacking interactions consolidated by noncovalent interactions in their solid phases. The electron reorganization energy for both molecules were determined smaller than that of holes which means they have n-type semiconductor properties. The charge transfer integrals were calculated with the optimization of molecules' dimer configurations that the theoretical results demonstrate the charge transfer integral depends on the distance between the stacking rings. High charge transfer integral and small reorganization energy give the high charge mobility for the semiconductor molecules. Beside the mobility, energy band gap, ionization potential, electron and hole injection barriers of the molecules were interpreted to further understand their electronic properties. Due to the small LUMO values which provide n-type molecule and small electron injection barrier. From our work both molecules can be effective n type organic semiconductor devices with the high mobility and can be modified for more efficient charge transport in phenanthroline derivatives.

2. Theoretical Methodology

Density functional theory studies are a widely used computational method to understand the optical and electronic properties of organic materials. B3LYP-6311G (d, p) basis set was used with the Gaussian 09 software in this study (Reed *et al.*, 2014). The optimized geometries of the neutral and charged states of the molecules were determined from cif file obtained by single crystal x-ray diffraction experiment. The charge transfer integral and reorganization energy, ionization potential and electron affinity, charge transfer rate and mobility of the molecules were calculated by the combination of DFT and Marcus electron theory formula given in the equation 1.

$$k = \frac{4\pi^2}{\lambda} \frac{1}{\sqrt{4\pi\hbar k_B T}} t^2 \exp\left(-\frac{\lambda}{4k_B T}\right) \quad (1)$$

The reorganization energy (λ) includes; inner reorganization energy includes the geometric changes in the molecules and is the modifications in the molecular geometry if an electron, is removed or added to a molecule. The inner reorganization energy is divided into two parts: λ^1 represents the geometry relaxation energy of one molecule from neutral to charged state, λ^2 represents the geometry relaxation energy from charged to neutral state (Yang *et al.*, 2019).

$$\lambda = \lambda_{rel}^1 + \lambda_{rel}^2 \quad (2)$$

In the evaluation of λ , the two terms were computed directly from the adiabatic potential energy surfaces.

$$\begin{aligned} \lambda_{anion} &= \lambda_{rel}^1 + \lambda_{rel}^2 = [E^{(0)}(M^-) - E^{(0)}(M)] + [E^{(1)}(M) - E^{(1)}(M^-)] \\ \lambda_{cation} &= \lambda_{rel}^1 + \lambda_{rel}^2 = [E^{(0)}(M^+) - E^{(0)}(M)] + [E^{(1)}(M) - E^{(1)}(M^+)] \end{aligned} \quad (3)$$

where $E^0(M^+)$ and $E^0(M)$ represent the energies of the neutral molecule at the cation geometry and at the optimal ground-state geometry respectively. $E^1(M)$ and $E^1(M^+)$ represent the energy of the charged state at the neutral geometry and optimal cation geometry, respectively. In the calculation of ionization energy, the adiabatic ionization potential (IPa) and vertical ionization potential (IPv), the adiabatic/vertical electron affinity (EAa)/(EAv) of both molecules have been calculated as the following equation.

$$\begin{aligned} IPa &= E^0(M)^+ - E^0(M) \text{ and } IPv = E^1(M)^+ - E^0(M) \\ EAA &= E^0(M) - E^0(M)^- \text{ and } EAV = E^0(M) - E^1(M)^- \end{aligned} \quad (4)$$

The charge transfer integral of the molecules was calculated by using the DFT optimized molecular configuration for its dimeric structure given in the Figure 2. Using the DFT optimized molecular configurations for dimeric structures of the molecule 1 and 2 created by the pi...pi stacking interactions, the charge transfer integral of the both molecules were determined. In the formation of the dimeric structure with two isolated molecules, two HOMO (LUMO) levels from each molecule combines to make HOMO and HOMO-1 (LUMO and LUMO+1) in a dimer. In a simplified energy splitting in dimer, the charge transfer integral (t) is approximated as the half of the energy difference between HOMO and HOMO-1 for hole transfer whereas LUMO and LUMO+1 for electron transfer. (Köse *et al.*, 2007)

$$t_{hole} = \frac{HOMO-HOMO-1}{2} \quad t_{electron} = \frac{LUMO-LUMO+1}{2} \quad (5)$$

To estimate the transfer integral of the molecules, we have taken into account perpendicular distances between the adjacent rings is 3.947 Å for the molecule 1 and 3.77 Å and 3.44 Å for the molecule 2. Two dimeric configurations were considered to calculate the charge transfer integral of the molecule 2. The formula of the diffusion coefficient associated to a one-dimensional jumping process is given in the equation 6.

$$D = K_B d^2 \quad (6)$$

The mobility, μ , can be obtained from the following expression where e is the electron charge d is the transport distance from the molecular center to center in a stacking dimer, k_B is the Boltzmann constant and T was taken 300 K (Huang *et al.*, 2020).

$$\mu = \frac{eD}{kT} = \frac{ed^2k_T}{k_B T} \quad (7)$$

3. Results and Discussion

3.1. Prediction of charge transport properties of the molecules

The crystal structure of the **molecule 1** (2,7-dibutylbenzo[*lmn*][3,8] phenanthroline-1,3,6,8(2H,7H)-tetrone) and **molecule 2** (2,7-dipropylbenzo[*lmn*][3,8]phenanthroline-1,3,6,8(2H,7H)-tetrone) were taken from Cambridge crystallographic database sample 819749 ($a = 5.2230(10)$ Å, $b = 7.840(2)$ Å, $c = 11.132(3)$ Å, $Z = 4$ and $\alpha = 103.716(2)^\circ$, $\beta = 94.279(2)^\circ$, $\gamma = 93.858(3)^\circ$) and sample 1029340 ($a = 6.9622(4)$ Å, $b = 17.2426(11)$ Å, $c = 27.5809(15)$ Å, $Z = 4$ and $\alpha = 90^\circ$, $\beta = 90^\circ$, $\gamma = 90^\circ$) (Huang *et al.*, 2020; Krishna *et al.*, 2016). We investigated the charge transfer and electronic characteristic of the both molecules in terms of their hole and electron reorganization energies, charge transfer integral, energy gap, ionization potential (IP) and electron affinity (EA) and charge mobility as shown in Table 1. The optimized structures in the neutral state of the both molecules are presented in the Figure 1.

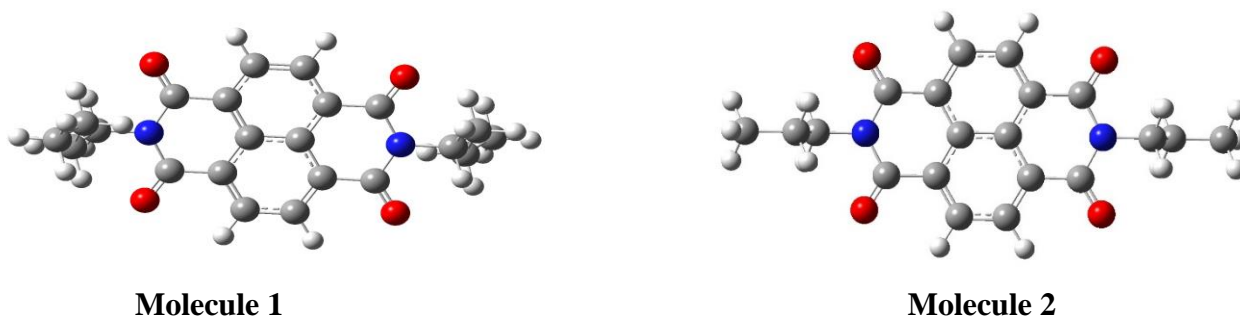


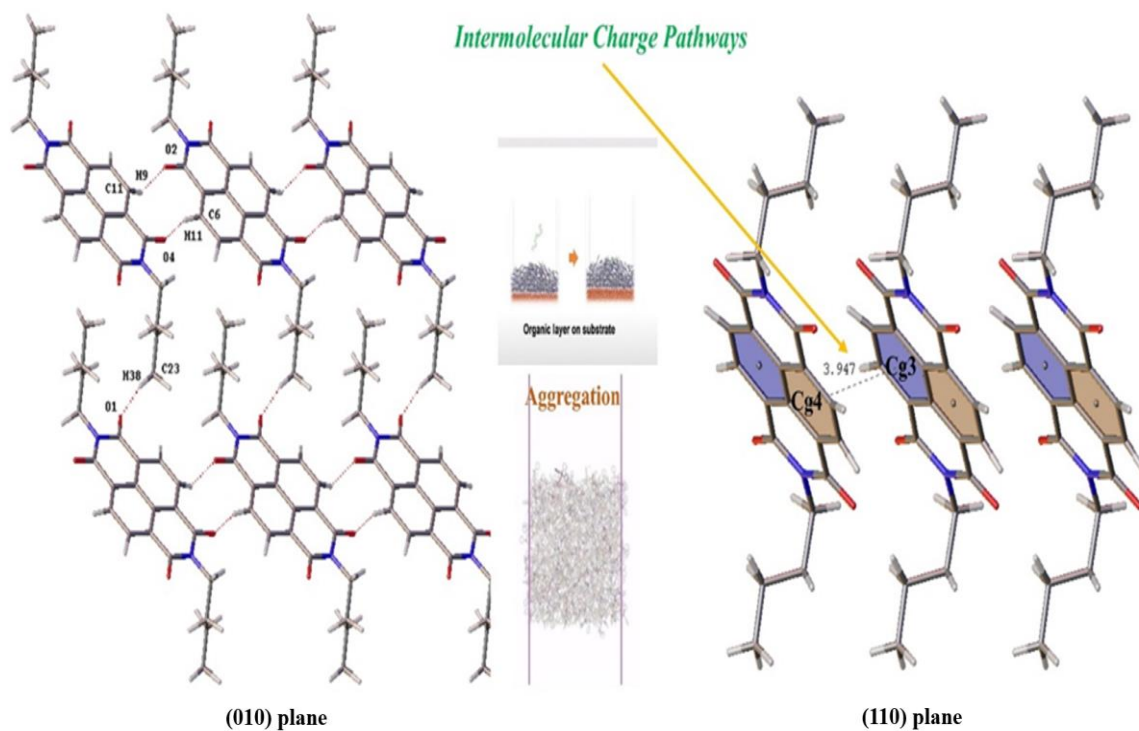
Figure 1. Optimized geometry of the molecules in the neutral state.

Table 1. The value of parameters determining the charge transfer property of the molecules.

| Molecule | λ_{hole} (eV) | $\lambda_{electron}$ (eV) | t_{elec} | t_{hole} | IPa (eV) | IPv (eV) | Ea (eV) | Ev (eV) | k_{hole} (s ⁻¹) | $k_{electron}$ (s ⁻¹) |
|----------|-----------------------|---------------------------|---|---|----------|----------|---------|---------|---|--|
| 1 | 2.39 | 0.0030 | 0.086 | 0.025 | 8.61 | 10.9 | 2.30 | 2.12 | 1.1×10^{12} | 3.5×10^{14} |
| 2 | 0.0037 | 0.0036 | 0.038 (dimer 1) 0.78 (dimer 2) | 0.016 (dimer 1) 0.14 (dimer 2) | 8.43 | 8.53 | 2.04 | 1.86 | 2.4×10^{13} 5.06×10^{15} | 3.34×10^{14} 1.54×10^{17} |

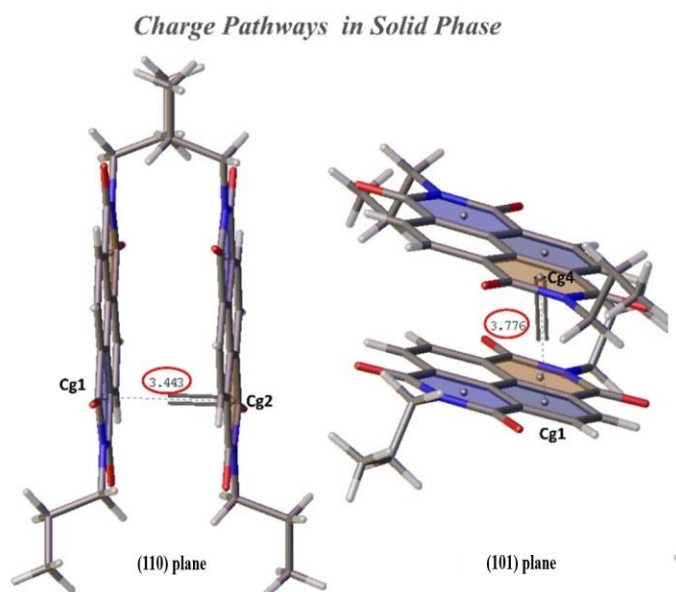
| Molecules | d_L (Å) | μ_{hole} (cm ² V ⁻¹ s ⁻¹) | $\mu_{electron}$ (cm ² V ⁻¹ s ⁻¹) |
|-----------|-----------|---|---|
| 1 | 3.947(3) | 0.066 | 21.13 |
| 2 | 3.77(2) | 1.3 | 18 |
| 2 | 3.44(2) | 11 | 70 |

Reorganization energies of the molecule 1 for hole and electron transfer were calculated from adiabatic potentials are 2.39 and 0.003 eV, respectively. The reorganization energies of molecule 2 are 0.0037 eV for hole and 0.0036 eV for electron. Because of lower electron reorganization energy, it is suggested that both molecules exhibit the higher intrinsic electron transfer rate, and hence, higher electron mobility than that of hole. Therefore, both molecules can be called n-type semiconductors. In terms of the dihedral angle in the crystal structure of the molecule 1 and 2 between the fragments we interpreted the reorganization energy. The dihedral angle for neutral state of molecule 1 is 76.95803 while this value was found as 79.33375 and 79.96829 for the cationic and anionic states, respectively. The cationic state



is more dominant than anionic state in terms of the dihedral angle between the two rings. It means that electron reorganization energy is smaller than those of the hole. The charge carriers could be electrons. This situation were observed in the molecule 2 that the diheral angles for the neutral, anion and cation state were found as 179.911° , 179.908° and 179.986° , respectively.

Molecule 1



Molecule 2

Figure 2. Hopping pathways within crystal structure of the molecule 1 and molecule 2.

Charge transport properties strongly depend on the solid-state packing arrangements and orientations of the molecules including noncovalent interactions such as van der Waals interactions, π - π stacking, and hydrogen bondings (Alvey *et al.*, 2010; Cheng *et al.*, 2016). The reported crystalline structures of the molecules based on the X-ray diffraction analysis show the packing of molecules with the typical J type stacking consolidated with C-O... π and nonclassical C-H...O hydrogen bonds in their solid phases. Charge transfer integrals were obtained by from the geometries of the dimers optimized (B3LYP/6-31G(d, p)) where the center of mass distance and the angle between molecular planes were fixed by freezing the coordinate of the central rings. Since the dimers are symmetric and two monomers are equivalent under the symmetric transformation in the charge transfer process we can neglect the electrostatic polarization effect (Swicka *et al.*, 2018; Tan *et al.*, 2021).

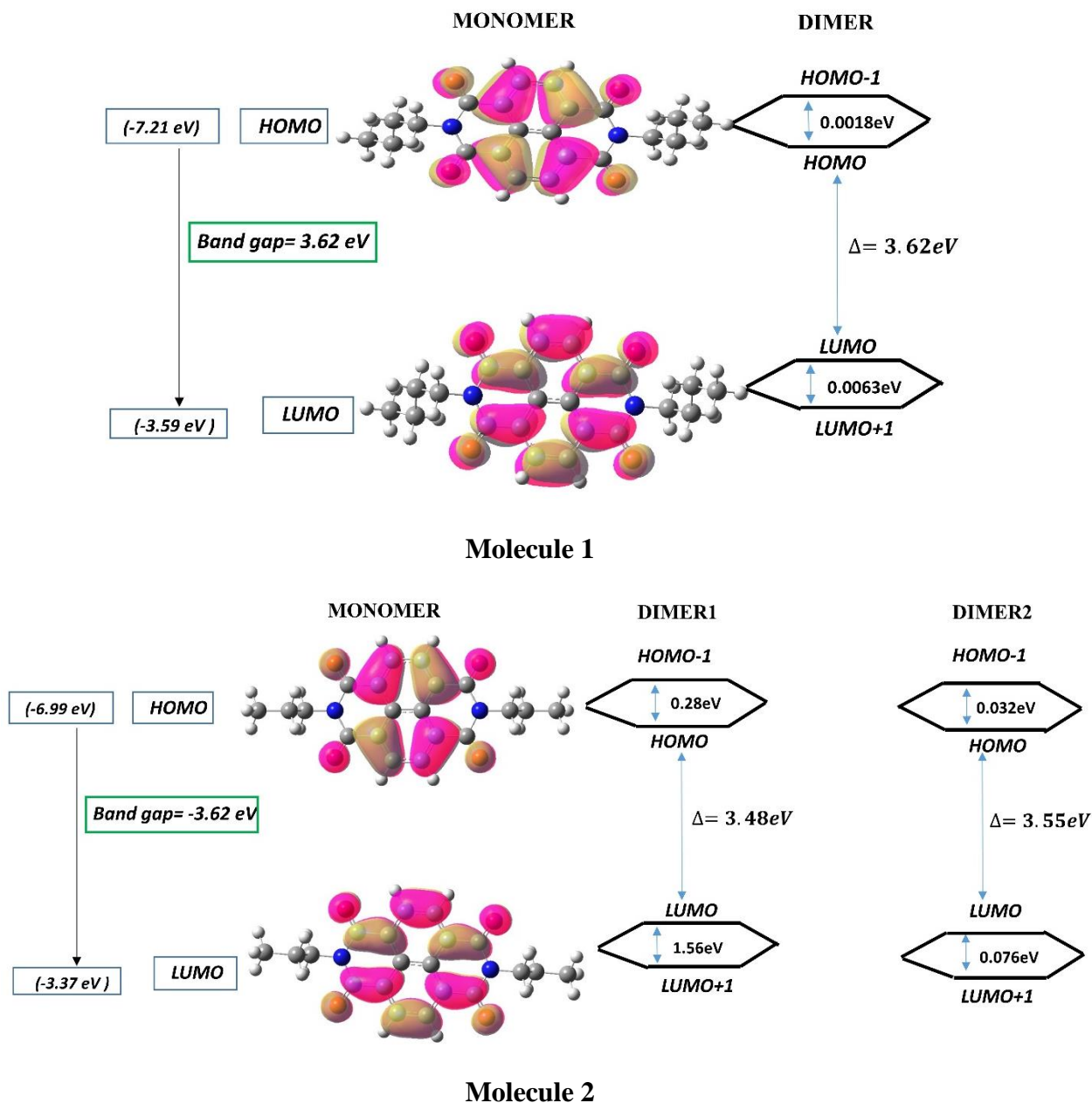


Figure 3. Energy level diagram of the frontier orbitals for dimers of the both molecules in solid phase.

Fig. 3 describes the energy level diagram of dimer of the molecule 1 along 110 plane shown in Fig. 2. LUMO and HOMO levels of two monomers were combined and created LUMO+1, LUMO, HOMO and HOMO-1 in the dimer configuration. Along 110 plane, the energy level splitting between HOMO and HOMO-1 is about 0.0018 eV. In contrast, the energy splitting between LUMO and LUMO+1 is 0.0063 eV, which is 3.5 times higher, indicating a poor hole transport in this material. For the dimer 1 of the molecule 2, the energy level splitting between HOMO and HOMO-1 is about 0.28 eV while that of LUMO and LUMO+1 is 1.5 eV which

supports molecule 2 is an efficient electron transfer molecule. This situation is valid for the dimer 2 of the molecule 2. The charge transfer integral value of the dimeric 2 configuration of the molecule 2 has the highest value of $70 \text{ cm}^2 \text{ V}^{-1} \text{ s}^{-1}$ due to the more stronger stacking interactions with the small perpendicular distance between the rings (3.44 \AA). This charge pathway creates efficient charge transport in the molecule 2 along the (110) plane. Electron mobility by considering the expression for the diffusion coefficient associated to a one-dimensional jumping process was found greater than hole mobility for each dimeric configuration of the molecules which supports they show n-type semiconductor material feature (Table 1).

The injection of the holes and electrons play an important role to create optimized electronic devices in real world (Yang *et al.*, 2008; Senevirathna *et al.*, 2014). The information about the organic device performance and its stability can be obtained from the parameters of ionization potential (IP) and electronic affinity (EA) that determine the charge injection through estimating the energy barrier for injection of hole and electron into molecule. The ionization energy describes the energy necessary to remove electrons from the neutral molecule to create cation molecule. The higher IP values indicate that the molecule is difficult to become cation in environment to react with OH^- (H_2O) or O_2^- (O_2) existing in the atmosphere. Hence, it is indicated that molecule 2 is more sensitive to the reaction with ion OH^- or O_2 . (Liu *et al.*, 2013; Huong *et al.*, 2013). While molecule 1 is more stable and hardly oxidized which can be favoured for the practical applications (Gruhn *et al.*, 2002).

The EA values of molecule 1 and molecule 2 are 2.30 and 2.04 eV, respectively (Table 1). For the devices if the EA value is high, it means that injection energy for electron will be small (commonly used metallic electrodes (3 eV)). From these EA values, we can see that molecule 1 is better than molecule 2 for transporting electrons from both lowering the energy barrier for electron injection. Besides that, the HOMO energy levels for both compounds are not good agreement with the work function of the gold electrode (-5.2 eV). Therefore, the injection of the hole from the gold to the organic semiconductor does not easily accomplished. For example, OFET is composed of a gate electrode, dielectric layer, organic semiconductor layer, and source-drain (S-D) electrodes. Carrier injection from the S-D electrode into the organic layer mainly depends on the barrier between the work function of the metal electrode and the HOMO or LUMO energy level of the organic semiconductors (Daswani *et al.*, 2018).

N-type materials, typically have LUMO levels between -3 and -4 eV and have better contact with low work-function metals, such as calcium and lithium. The LUMO levels are 3.37 eV and 3.59 eV for both molecules.

4. Conclusions

Molecular packing in organic materials greatly influences the charge mobility in organic light-emitting diodes (OLEDs), organic photovoltaics (OPVs), and organic field-effect transistors (OFETs). Here, we have performed the calculation of the charge mobility in molecular crystals of phenanthroline derivatives by considering the reorganization energy for the monomer molecules and charge transfer integral for the dimeric configurations of the molecules. With the combination of density functional theory and Marcus Charge Transfer Theory. The drift electron mobility of the molecule **1** and **2** were determined to $21.13 \text{ cm}^2 \text{ V}^{-1} \text{ s}^{-1}$ and $18.00 \text{ cm}^2 \text{ V}^{-1} \text{ s}^{-1}$, respectively through J type $\pi \cdots \pi$ stacking interactions created by small perpendicular distances between the adjacent rings. The electron reorganization energy for both molecules were determined smaller than that of holes which means they have n-type semiconductor properties. Due to the small LUMO values which provide n-type molecule and small electron injection barrier for the molecules. Molecule **2** is more sensitive to the reaction with ion OH^- or O_2 while molecule **1** is more stable and hardly oxidized which can be favoured for the practical applications due to the high ionization potential of the molecule **1**. Electron mobility by considering the expression for the diffusion coefficient associated to a one-dimensional jumping process was found greater than hole mobility for each dimeric configuration of both molecules which supports they show n-type semiconductor material feature. From our work both molecules can be effective n type organic semiconductor devices with the high mobility and can be modified for more efficient charge transport in phenanthroline derivatives for applications in real world.

Acknowledgement

The author acknowledges Assoc. Prof. Dr. Muhittin Aygün studying at Dokuz Eylül University for technical contribution

Author contributions

Gül Yakalı wrote the whole manuscript and with Zeynep Türkmen Bulca performed and interpreted theoretical calculations.

Declarations

Conflict of interest

The authors declare that they have no conflict of interest.

Funding

The authors received no specific funding for this work.

References

Alvey P. M., Reczek J. J., Lynch V., and Iverson B. L. 2010. A Systematic Study of Thermochromic Aromatic Donor-Acceptor Materials. *J. Org. Chem.*, 75, 7682–7690.

Chai S., Wen S., Huang J., and Han K. 2011. Density Functional Theory Study on Electron and Hole Transport Properties of Organic Pentacene Derivatives with Electron-Withdrawing Substituent. *Journal of Computational Chemistry*, 3218-3225.

Chakravarty M. and Vora A., 2021. *Drug Delivery and Translational Research*, 11, 748.

Chang Y. and Chao I. 2010. An Important Key to Design Molecules with Small Internal Reorganization Energy: Strong Nonbonding Character in Frontier Orbitals. *J. Phys. Chem. Lett.*, 1, 116–121.

Cheng Y., Qi Y., Tang Y., Zheng C., Wan Y., Huang W., and Chen R. 2016. Controlling Intramolecular Conformation Through Nonbonding Interaction for Soft-Conjugated Materials: Molecular Design and Optoelectronic Properties. *J. Phys. Chem. Lett.*, Just Accepted Manuscript.

Cias P., Slugovc C., and Gescheidt G. 2011. Hole Transport in Triphenylamine Based OLED Devices: From Theoretical Modeling to Properties Prediction. *J. Phys. Chem. A*, 115, 14519–14525.

Daswani U., Singh U., Sharma P., and Kumar A. 2018. From Molecules to Devices: A DFT/TD-DFT Study of Dipole Moment and Internal Reorganization Energies in Optoelectronically Active Aryl Azo Chromophores. *J. Phys. Chem. C*, Just Accepted Manuscript.

Gao H. 2010. Theoretical investigation into charge mobility in 4,40-bis(1-naphthylphenylamino) biphenyl. *Theor. Chem. Acc.* 127:759–763.

García-Frutos E. M., Gutierrez-Puebla E., Monge M. A., Ramírez R., Andrés P., Andrés A., Ramírez R., Gómez-Lor B. 2009. Crystal structure and charge transport properties of N-trimethyltriindole: Novel p-type organic semiconductor single crystals. *Organic Electronics* 10 643–652.

Gruhn N. E., Silva Filho D. A., Bill T. G., Malagoli M., Coropceanu V., Kahn A., and Bre´das J. 2002. The Vibrational Reorganization Energy in Pentacene: Molecular Influences on Charge Transport. *J. Am. Chem. Soc.*, 124, 7918-7919.

Huang W., Xie W., Huang H., Zhang H., and Liu H. 2020. Designing Organic Semiconductors with Ultrasmall Reorganization Energies: Insights from Molecular Symmetry, Aromaticity and Energy Gap. *J. Phys. Chem. Lett.*, Just Accepted Manuscript.

Huong V. T. T., Nguyen H. T., Tai T. B., and Nguyen M. T. 2013. π -Conjugated Molecules Containing Naphtho[2,3-b]thiophene and Their Derivatives: Theoretical Design for Organic Semiconductors. *J. Phys. Chem. C*, 117, 10175–10184.

Hutchison G. R., Ratner M. A., and Marks T. J. 2005. Intermolecular Charge Transfer between Heterocyclic Oligomers. Effects of Heteroatom and Molecular Packing on Hopping Transport in Organic Semiconductors. *J. Am. Chem. Soc.*, 127, 16866-16881.

Irfan A., Al-Sehemi A. G., Aijaz Rasool Chaudhry A. R., Muhammad S. 2018. The structural, electro-optical, charge transport and nonlinear optical properties of oxazole (4Z)-4-Benzylidene-2-(4-methylphenyl)-1,3-oxazol- 5(4H)-one derivative. *Journal of King Saud University – Science* 30, 75–82.

Jia X., Wei H., Shi Y., Liu Y. 2019. Theoretical studies on charge transport and optical properties of diarylmaleic anhydride derivatives as organic light-emitting materials. *Chemical Physics Letters* 724 50–56.

Köse M. E., Mitchell W. J., Kopidakis N., Chang C. H., Shaheen S. E., Kim K., and Rumbles G. 2007. Theoretical Studies on Conjugated Phenyl-Cored Thiophene Dendrimers for Photovoltaic Applications. *J. AM. CHEM. SOC.*, 129, 14257-14270.

- Krishna G. R., Devarapalli R., Lal G., and Reddy C. M. 2016. Mechanically Flexible Organic Crystals Achieved by Introducing Weak Interactions in Structure: Supramolecular Shape Synthons. *J. Am. Chem. Soc.*, 138, 13561–13567.
- Li H X, Wang X F, Li Z F. 2012. Theoretical study of the effects of different substituents of tetrathiafulvalene derivatives on charge transport. *Chin Sci Bull*, 57: 4049-4056.
- Liu Y., Sun X., Gahungu G., Qu X., Wang Y. and Wu Z. 2013. DFT/TDDFT investigation on the electronic structures and photophysical properties of phosphorescent Ir (III) complexes with conjugated/non-conjugated carbene ligands. *J. Mater. Chem. C*, 1, 3700.
- McMahon D. P. and Troisi A. 2010. Evaluation of the External Reorganization Energy of Polyacenes. *J. Phys. Chem. Lett.*, 1, 941–946.
- Navamani K., Saranya G., Kolandaivel P. and Senthilkumar K. 2013. Effect of structural fluctuations on charge carrier mobility in thiophene, thiazole and thiazolothiazole based oligomers. *Phys.Chem. Chem. Phys.*15, 17947.
- Nguyen T. P., Shim J. H., and Lee J. Y. 2015. Density Functional Theory Studies of Hole Mobility in Picene and Pentacene Crystals. *J. Phys. Chem. C*, Just Accepted Manuscript.
- Reed A. E., Carpenter J. E., and Weinhold F. 2014. NBO Version 3.1, E. D. Glendening.
- Senevirathna W., Daddario C. M., and Sauvé G. 2014. Density Functional Theory Study Predicts Low Reorganization Energies for Azadipyrromethene-Based Metal Complexes. *J. Phys. Chem. Lett.*, 5, 935–941.
- Siddiqui S. A., Al-Hajry A., and Al-Assiri M. S. 2016. Ab Initio Investigation of 2,20-Bis(4-trifluoromethylphenyl)- 5,50-Bithiazole for the Design of Efficient Organic Field-Effect Transistors. *International Journal of Quantum Chemistry*, 116, 339–345.
- Swicka S. M., Zhua W., Mattaa M., Aldricha T. J., Harbuzaruc A., Navarretec J. T. L., Ortizc R. P., Kohlstedta K. L., Schatza G. C., Facchettia A., Melkonyana F. S., and Marks T. J. 2018. Closely packed, low reorganization energy π -extended postfullerene acceptors for efficient polymer solar cells. *PNAS Latest Articles*.

Tan Y., Casetti N. C., Boudouris B. W., and Savoie B. M. 2021. Molecular Design Features for Charge Transport in Nonconjugated Radical Polymers. *J. Am. Chem. Soc.*, 143, 11994–12002.

Tripathi A., Prabhakar C. 2019. Optoelectronic and charge-transport properties of truxene, isotruxene, and its heteroatomic (N, O, Si, and S) analogs: A DFT study. *J Phys Org Chem.*; 32: e3944.

Wang C., Dong H., Jiang L. and Hu W. 2018. Organic semiconductor crystals. *Chem. Soc. Rev.*, 47, 422.

Wang L., Duan G., Ji Y., and Zhang H. 2012. Electronic and Charge Transport Properties of peri- Xanthenoxanthene: The Effects of Heteroatoms and Phenyl Substitutions. *J. Phys. Chem. C*, 116, 22679–22686.

Wang L., Li T., Shen Y., and Song Y. 2016. A theoretical study of electronic structure and charge transport property for thieno[2,3-b] benzothiophene based derivatives. *Phys. Chem. Chem. Phys.* Qi Y., Chen C., Zheng C., Tang Y., Wan Y., Jiang H., Chen T., Tao Y. and Chen R. 2020. Heteroatom-bridged Heterofluorenes: A Theoretical Study on Molecular Structures and Optoelectronic Properties *Phys. Chem. Chem. Phys.*, 00, 1-3.

Yan L., Zhao Y., Yu H., Hu Z., He Y., Li A., Goto O., Yan C., Chen T., Chen R., Loo L., Perepichka D., Meng H. and Huang, W.J. 2013. Influence of Heteroatoms on the Charge Mobility of Anthracene Derivatives. *J. Name.*, 00, 1-3 | 1.

Yang L., Mao J., Yin C., Mohamad A. A., Wu X., Dong C., Liu Y., Wei Y., Xie L., Ran X. and Huang W. 2019. Novel Structure of Grid Spirofluorene: A New Organic Semiconductor with Low Reorganization Energy. *J. Name.*, 2013, 00, 1-3 | 1.

Yang X., Wang L., Wang C., Long W., and Shuai Z. 2008. Influences of Crystal Structures and Molecular Sizes on the Charge Mobility of Organic Semiconductors: Oligothiophenes. *Chem. Mater.*, Vol. 20, No. 9.

Zhang D., Xu F., Lu Q., Zhang R., Xia J. 2023. Poly(3-amino-carbazole) derivatives containing 1,10-phenanthroline and 8-hydroxyquinoline ligands: Synthesis, properties and application as ion sensors. *Spectrochimica Acta Part A: Molecular and Biomolecular Spectroscopy*, Vol. 295.

Zhang M. and Zhao G. 2012. Heteroatomic Effects on Charge-Transfer Mobility of Dianthra [2,3-b:2',3'-f] thieno[3,2-b] thiophene (DATTT) and Its Derivatives. *J. Phys. Chem. C*, 116, 19197–19202.

Zhu R., Duan Y., Geng Y., Wei C., Chen X., Liao Y. 2016. Theoretical evaluation on the reorganization energy of five-ring-fused benzothiophene derivatives. *Computational and Theoretical Chemistry* 1078 16–22.

Zhang Y., Cai X., Bian Y., Li X., and Jiang J. 2008. Heteroatom Substitution of Oligothienoacenes: From Good p-Type Semiconductors to Good Ambipolar Semiconductors for Organic Field-Effect Transistors. *J. Phys. Chem. C*, 112, 5148-5159.